Materials Chemistry and Physics 270 (2021) 124823

Contents lists available at ScienceDirect

Materials Chemistry and Physics

journal homepage: www.elsevier.com/locate/matchemphys

Ordered graphitized ceramic layer induced by liquid crystal epoxy resin in silicone rubber composites with enhanced ablation resistance performance

Zhuodong Liu, Ziyang Chen, Liwei Yan, Yang Chen *, Mei Liang, Huawei Zou **

The State Key Lab of Polymer Materials Engineering, Polymer Research Institute of Sichuan University, Chengdu, 610065, China

HIGHLIGHTS

- The average ablation rate was reduced significantly.
- The liquid crystal led to more orderly graphitic carbon structures during pyrolysis.
- The liquid crystal component increased the strength of the ceramic layers.
- More holes generated could prevent the flame from spreading to deeper layers of the sample.

ARTICLE INFO

Keywords:
Silicone rubber
Ablation resistance
Ceramization process
Flexible ablation matrix

ABSTRACT

In ablation-resistant silicone rubber composites, the strengths of the ceramic layers strongly affect the ablation rates of the materials, and the order of graphite carbon in the ceramic layers has an important impact on the strength of ceramic layers. In this study, a series of 4,4′-bis(3-(oxiran-2-ylmethoxy)benzyl)-1,1′-biphenyl(BER) modified silicone rubber composites were prepared to improve the order of graphite carbon in the ceramic layers of composites after ablation. The introduction of SiO_2 nanoparticles and carbon fibers as ablation fillers made the material ceramized and formed strong ceramic layers during the ablation process. Characterization of ablation performance shown that the 20BER composite exhibited the best ablation resistance performance: a linear ablation rate of 0.0464 mm/s and a mass ablation rate of 0.0500 g/s. Mechanical performance characterization shown that the 20BER sample also exhibited an excellent tensile strength of 2.013 MPa and a ceramic layer strength of 13.15 MPa. Raman measurement indicated that the addition of BER led to more orderly graphitic carbon structures during pyrolysis and increased the strength of ceramic layers. SEM, mercury intrusion and thermal conductivity measurements indicated that the pore volume, porosity and total pore area of ceramic layers with the BER component were all higher than the 0BER sample. The BER was proven to be an effective material which is beneficial to improve the ablation resistance and played an important role in the process of ceramization of the silicone rubber composites. These silicone rubber composites have the potential to be applied to the surface coating of aircraft.

1. Introduction

Ablation materials are important materials which ensure the normal flight of spacecraft. Ablation materials can generally be divided into rigid ablation materials and flexible ablation materials, they are often used as the inner thermal insulation layer of spacecraft engines, the combustion-limiting coating of propellants and the nozzle throat lining of rocket engines [1,2]. With the continuous improvement of the flying speed of high-performance aircraft, the thermal environment of the elastomer structural components and the engine casing that ensure the normal operation of the engine is getting worse, mainly manifested in the increase of heat flow density and serious aerodynamic erosion. Higher requirements are put forward for the heat-proof coating outside the engine casing. Due to the unsatisfactory aging resistance, air tightness, brittleness temperature and elongation of rigid materials, in recent years, flexible ablation materials, especially ceramic silicone rubber as a

* Corresponding author.
** Corresponding author.
E-mail addresses: 404197778@qq.com (Z. Liu), 2926034476@qq.com (Z. Chen), liweiyan68@163.com (L. Yan), cy3262276@163.com (Y. Chen), liangmeiww@163.com (M. Liang), hwzou@163.com (H. Zou).

https://doi.org/10.1016/j.matchemphys.2021.124823
Received 17 January 2021; Received in revised form 27 May 2021; Accepted 3 June 2021
Available online 6 June 2021

new type of fire-retardant composite material has become a research hotspot [3,4].

Ceramic silicone rubber is a silicone rubber-based fire-retardant composite material made by adding ceramic filler, flux or reinforcing agent and other inorganic fillers to the silicone rubber matrix [4–7]. Ceramization process is characterized by creation of stiff, durable and porous ceramic structure from highly filled polymer composite during heat treatment to block propagation of flames and preventing burning material from deeper penetration of oxygen [8]. Pure silicone rubber can only generate flocculent SiO_2 during the ablation process, but cannot form a strong ceramic layer, so it is difficult to apply in practical work. In order to increase the residual weight of materials and promote the formation of a strong ceramic layer after ablation, many methods have been reported for silicon rubber ablation composite materials, such as adding SiO_2 as a ceramic filler and adding carbon fiber, hafnium oxide (HfO_2) [9], zirconium carbide (ZrC) and zirconia (ZrO_2) [10] or other fibers as fluxing agents. Besides SiO2 and carbon nanomaterials, aluminosilicate clay nananoparticles such as modified halloysite nanotubes (HNTs) [11–13] can be effective as fillers for silicon rubbers and natural resins. The ceramic silicon rubber ablation materials modified by these methods show excellent ability to withstand fast-flowing high-temperature combustion gases and plays an important role in reducing the temperature rise of the rocket engine casing [14]. However, simply adding fibers to modify the ablation materials may reduce the processability of the material and increase the cost.

Studies have shown that the formation of more ordered graphitic carbon during the ablation process can help increase the strength of the ceramic layers, thereby improving the ablation performance of the materials. Many methods have been proposed such as adding graphene [15], nano carbon black [16] and MWCNTs [17,18] to the silicone rubber matrix. However, these carbon-based materials will increase the thermal conductivity of the ceramic layer after ablation, and adversely affect the ablation rate of the material. 4,4′-bis(3-(oxiran-2-ylmethoxy) benzyl)-1,1′-biphenyl(BER) is a kind of self-flammable biphenol epoxy resin with a rigid molecular structure and a melting point of about 100 °C, which is easy to mold. Because of its excellent flame retardancy, excellent adhesion and high heat resistance, it is often used in electronic component packaging materials, solder mask inks, heat-resistant materials, molding materials and coatings, etc [19]. There have been some studies on the graphitization process of liquid crystal polymers, such as preparing high-performance carbon fiber through mesophase pitch liquid crystal [20–22]. It shows that liquid crystal is a high-quality carbon precursor and can form carbonization with a higher degree of graphitization during its liquid carbonization process. The graphitized structure is conducive to improving the oxidation resistance and structural toughness of ablation resistant materials. However, the application of liquid crystal modified silicone rubber ablative composites has not been reported until now, which may be a useful method to increase the ordered graphitic carbon content of silicone rubber composites after ablation. Starting from the design of the carbon layer structure during the ablation process, it is of great significance to find a new strengthening mechanism for the carbon layer and to develop a liquid crystal phase modified silicone rubber ablation composite material.

In order to further improve the ablation performance of silicone rubber ablation composites, in this paper, silicone rubber composites with silica (SiO_2) and carbon fibers, containing different content of BER were prepared. The mechanical performance of the composites were investigated in detail. The mechanism of the action of biphenol epoxy resin components in composite materials was also demonstrated by characterizing the morphology and performance of the carbon layers after ablation.

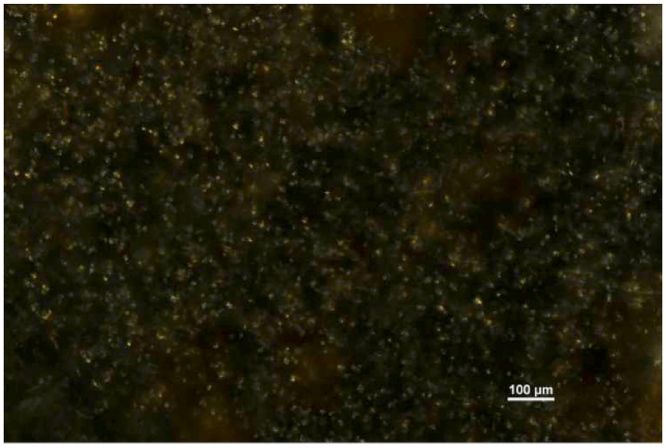

Fig. 1. Polarized light microscope image of liquid crystal BER.

2. Materials and methods

2.1. Materials

The silicone rubber used as the matrix in this study is a polydimethylsiloxane, which was modified by phenolic epoxy resin, coupling agent silicone intermediate (L-PMPS) and curing agent γ-aminopropyl triethoxysilane (KH550), all of which were from Zhonglan Chenguang Chemical Research & Design Institute Co., Ltd. (China). The BER was from Jiashengde Material Technology Co., Ltd. (China), which polarized light microscope image is shown in Fig. 1. It can be seen a clear liquid crystal texture in this image. The catalyst dibutyltin dilaurate (DBTDL) was from Chengdu Kelong Chemical Reagent Factory (China) and the filler SiO_2 nanoparticles and carbon fibers (3 mm) were obtained from Toho Chemical Co., Ltd (Japan).

2.2. Preparation of silicone rubber composites

The synthetic method of the epoxy system was from commercially available. A certain percentage of phenolic epoxy resin, L-PMPS and polydimethylsiloxane were mixed uniformly in a 2000 mL beaker as the matrix. Subsequently, the BER was stirred with the silicone rubber matrix at 120 °C till the BER was melted and dispersed evenly in the matrix. Next, SiO_2 nanoparticles were added to the mixture of silicone rubber and BER and mixed twice with a three-roll mill. Then, the carbon fibers, curing agent and catalyst were added to the mixture in turn and stirred uniformly. Finally, the mixed system was put into the mold and pressed in a cold press at a pressure of 10 MPa at room temperature for 24 h. The dimension of the ablation specimens was 30 mm × 10 mm (diameter × thickness) and the dimension of the tensile specimens was from GB T 528–2009 Standard for determination of tensile stress-strain properties of vulcanized rubber or thermoplastic rubber. Concentrations of BER in the samples were chosen to be 0, 5, 10, 15 or 20 wt% and the samples were referred to as 0BER, 5BER, 10BER, 15BER and 20BER, respectively. For comparison, silicone rubber without any filler was also prepared using the same procedures.

2.3. Characterizations

The ablative properties of the samples were measured using an oxyacetylene ablation machine (ZR-323A, Zhirui Co., China). A heat flux of 4152.9 kW/m^{-2} was created in the test and the burning time of each sample lasted 30s. The conditions of the ablation experiment referred to GJB 323A-1996. The distance between the sample surface and the flame nozzle (inner diameter: 2.0 mm) was 10 mm. The linear ablation rates and mass ablation rates were calculated by dividing the reduced thickness and mass of the samples by the ablation time of the samples. The

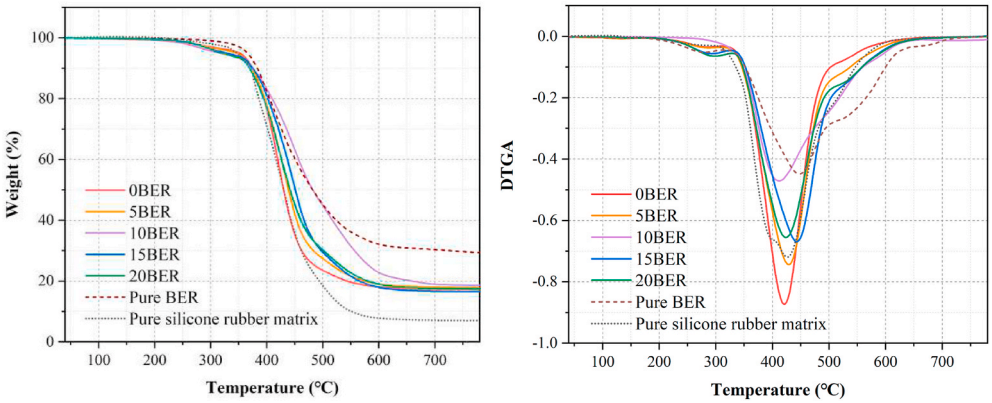

Fig. 2. TGA (a) and DTGA (b) curves of silicone rubber composites.

Table 1
DTGA peak temperature of silicone rubber composites.

Sample	0BER	5BER	10BER	15BER	20BER	Pure BER	Pure silicone rubber matrix
DTGA peak temperature(°C)	420	430	412.5	442.5	425	447.5	430

thermal stabilities of the materials from 35 to 800 °C in N_2 were characterized by a thermogravimetric analyzer (TG209F1, Netzsch Co., Germany) at a heating rate of 10 °C/min and a gas flow of 20 mL/min. The morphologies of the silicone rubber composites before and after ablation were characterized by a scanning electron microscope (S-4800, Hitachi Co., Japan) with an acceleration voltage of 5–15 kV. X-ray diffraction (XRD) patterns of the ceramic layer were collected using an X-ray diffractometer, (Ultima IV, Rigaku Co., Japan) with Cu K_α radiation (k = 0.1541 nm, 40 kV and 40 mA) in the 2θ range of 2–70° in reflection. The thermal conductivities of the ceramic layers were measured using a thermal conductivity analyzer (2500-OT, Hot Disk Co., Sweden). The tensile strength of the silicone rubber composites and the compressive strengths of the ceramic layers were measured using a universal material testing machine (5966, Instron Co., USA). The Mercury injection tests of the ceramic layers were using an automatic mercury porosimeter (AutoPore IV 9500, Micromeritics Co., USA). Raman measurements were measured using a Raman spectrometer (inVia Reflex, Renishaw Co., USA) and a laser wavelength of 532 nm was used as the excitation source.

3. Results and discussion

3.1. Thermal performance of the silicone rubber composites before ablation

The TGA and DTGA results are shown in Fig. 2 and were used to characterize the thermal stabilities of the silicone rubber composites and the BER. As Fig. 2(a) shows, the pure silicone rubber matrix has a residual weight of only 7.01%, and the pure BER has a residual weight of 29.21%. After adding SiO_2 and carbon fiber, the residual weight of the silicone rubber composite material had a certain increase compared with pure silicone rubber. However, with the increase of the BER content, the thermal weight loss of the five composites did not change significantly, and the residual weight of them was all around 18%. This indicated that the increase in the residual weight of the composites was mainly caused by SiO_2 and carbon fiber, and the BER has almost no effect on the residual weight. As the DTGA curves shows in Fig. 2(b), the silicone rubber composites before ablation started pyrolysis at 250 °C and reached the maximum weight loss rate at 400–450 °C, while the pure BER started pyrolysis at 450 °C. The pyrolysis temperature of the composites were not affected by the BER content. The DTGA peak temperature of all samples were listed in Table 1.

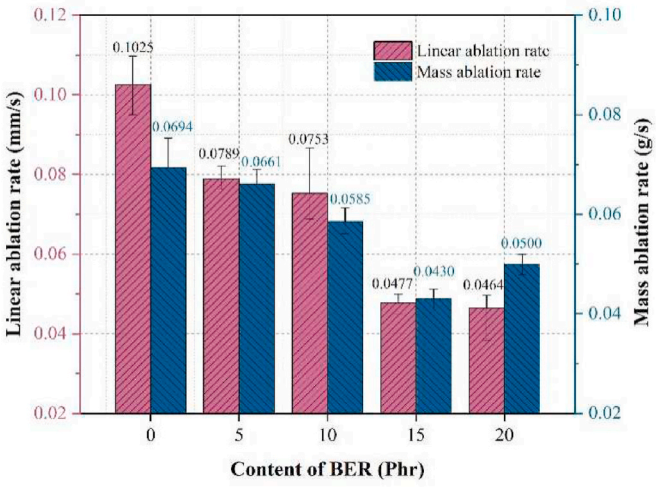

Fig. 3. Linear ablation rates and mass ablation rates of silicone rubber composites.

3.2. Ablation resistance of the silicone rubber composites

The linear ablation rates and the mass ablation rates obtained by dividing the thickness of the composites by the ablation time are plotted in Fig. 3. As the BER content increases, the linear ablation rate and mass ablation rate decrease significantly. The linear ablation rates for 0BER, 5BER, 10BER, 15BER and 20BER composites were 0.1205 mm/s, 0.0680 mm/s, 0.0605 mm/s, 0.0477 mm/s and 0.0464 mm/s, respectively, and the mass ablation rates for the five composites were 0.0684 g/s, 0.0599 g/s, 0.0533 g/s, 0.0430 g/s, 0.0500 g/s, respectively. At a BER concentration of 20 wt%, the average linear ablation rate was reduced by 54.7% and the average mass ablation rate was reduced by 30.0% compared to those of the 0BER, indicating that the addition of the BER effectively improved the ablation performance of the composites.

Fig. 4 shows the morphologies of the surfaces, sides and ceramic layers of silicon rubber composites after ablation. The ablation center of each sample was sunken and the surface was dense without large holes. The white powder covering the surface of the sample came from the original SiO_2 in the samples and the SiO_2 formed during the ablation

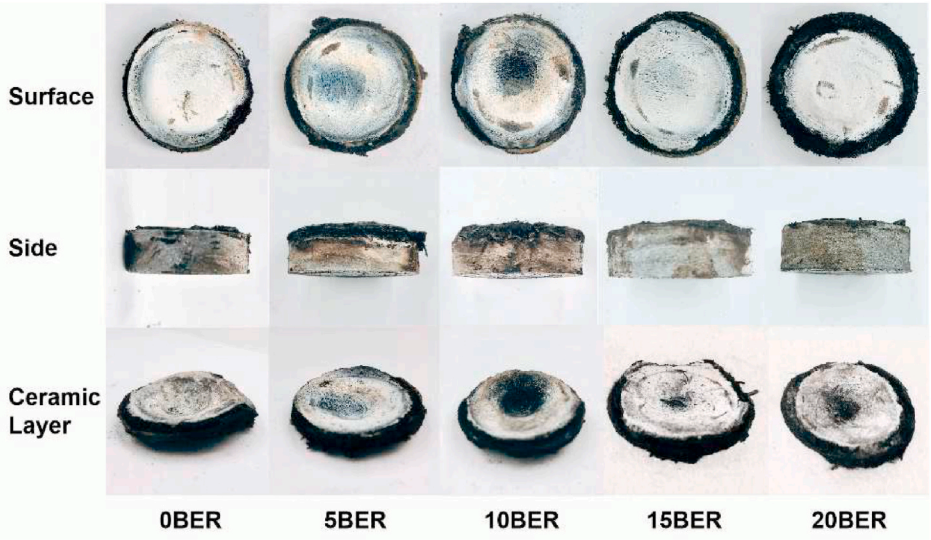

Fig. 4. Morphologies of the surfaces, sides and ceramic layers of silicon rubber composites after ablation. (For interpretation of the references to colour in this figure legend, the reader is referred to the Web version of this article.)

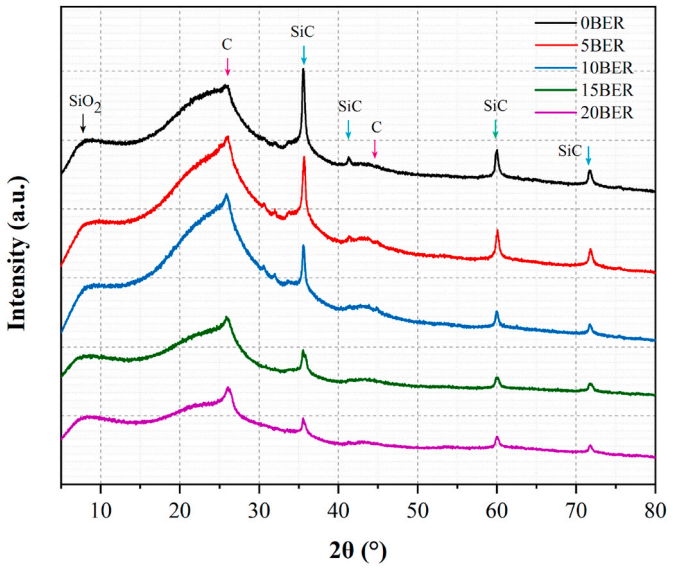

Fig. 5. XRD curves of the ceramic layers of composites.

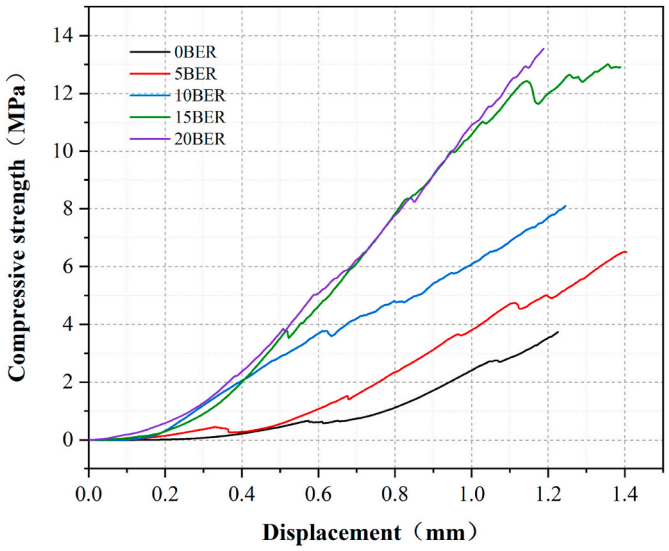

Fig. 6. Compressive strength-displacement curves obtained from compressive experiments.

process. It can be seen from the side morphologies that the ceramic layers and the material matrix were firmly bonded. The ceramic layers were completely peeled off from the substrate, indicated that the ceramic layers had good strength. In addition, carbon layers can not be seen on the side of the 15BER and 20BER samples, indicating that these two composites has a certain inhibitory effect on the flame propagation during the ablation process.

XRD analysis was used to characterize the composition of the silicon rubber ceramic layers of the composites after ablation. Fig. 5 shows the XRD curves of the ceramic layers. It can be seen that the ceramic layers after ablation of the five composites exhibited characteristic peaks at 8.0°, 26.2°, 35.6°, 41.9°, 43.8° , 60.1° and 72.5°. Among them, peaks at 35.6°, 41.9°, 60.1° and 72.5° are the characteristic peaks of SiC, indicating that the ceramization reaction occurred during the ablation process and the ceramic substance SiC was produced. Peaks at 43.8° and 26.2°are the characteristic peak attributable to C, which was attributed to the carbon residue produced during the ablation process. The characteristic peaks of SiO_2 at 8.0° were attributed to the SiO_2 nanoparticles contained in the composites and a small amount of SiO_2 newly produced during ablation. As the BER content increases, the intensity of the peaks in the figure tends to decrease. This is due to the decrease in the mass percentage of the silicone rubber matrix component, so the mass percentage of the generated ceramic substance also decreased.

Table 2
Compressive strength and modulus of ceramic layers after ablation of composites.

Sample	0BER	5BER	10BER	15BER	20BER
Compressive strength(MPa)	3.768	4.991	7.726	10.339	13.150
Compression modulus(MPa)	17.734	20.638	20.821	43.582	54.139

3.3. Ablation mechanism of the silicone rubber composites

The compression test was used to characterize the strength of the ceramic layers of the silicone rubber composites. One of the compressive strength-displacement curves of each sample is displayed in Fig. 6, and

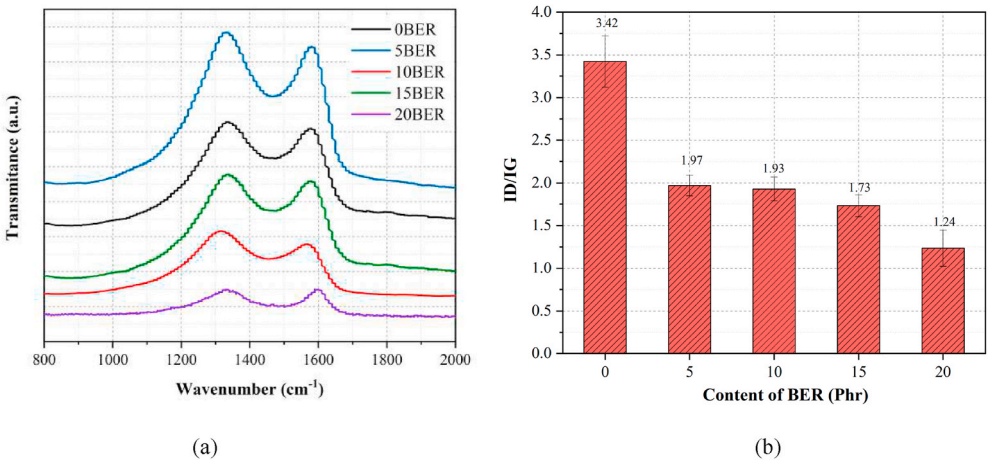

Fig. 7. Raman curves(a) and ID/IG values(b) of ceramic layers of composites.

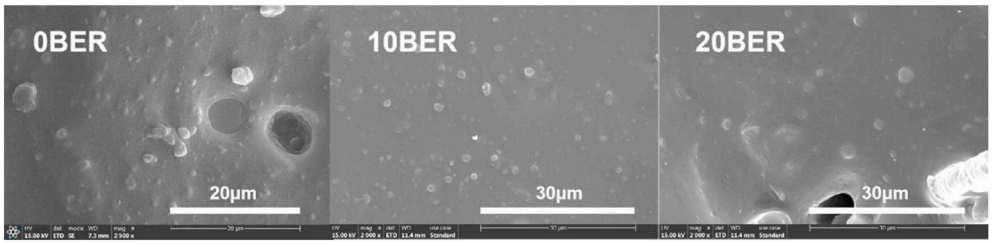

Fig. 8. Sectional morphologies of the silicone rubber composites before ablation.

the average compressive strengths and modulus of all ceramic layers are listed in Table 2. Compared with the 0BER sample, the compressive strengths of others were increased from 1.509 MPa to 1.534 MPa, 1.673 MPa, 1.912 MPa and 3.372 MPa, respectively, and the compressive modulus were increased from 17.734 MPa to 20.638 MPa, 20.821 MPa, 43.582 MPa and 54.139 MPa, respectively, with the increase of the BER content. This shows that the addition of BER components was beneficial to enhance the strength and modulus of the ceramic layers after ablation of the composites. With reference to the results of linear ablation rates and mass ablation rates, the strong ceramic layer formed during the ablation process might effectively resist the flame from further ablating the remaining part, thereby achieving the purpose of reducing the linear ablation rates and the mass ablation rates.

In order to further explore the reason for the increase in the strength of the ceramic layer, raman spectrum was tested to investigate the graphitic structures. The raman spectra curves of five composites are shown in Fig. 7(a). All samples show a D band around 1340 cm^{-1} corresponding to the disorder-induced phonon mode owing to defects and crystal boundaries and a G band near 1570 cm^{-1} exhibiting bond-stretching of sp [2] hybridized carbon atoms of ordered graphite structures [23]. The ratio of intensities of D to G bands (ID/IG), corresponding to the metric of "an amount of crystal boundary" or a disorder of graphitic structure [24]. ID/IG values were calculated after peak deconvolution of the D and G band by fitting with the Lorentzian function and were shown in Fig. 7(b). The smaller the ID/IG value, the better the order of graphitic carbon. ID/IG values of the samples containing BER (5BER, 10BER, 15BER and 20BER) are smaller noticeably compared to that of BER0, indicating that addition of BER led to more

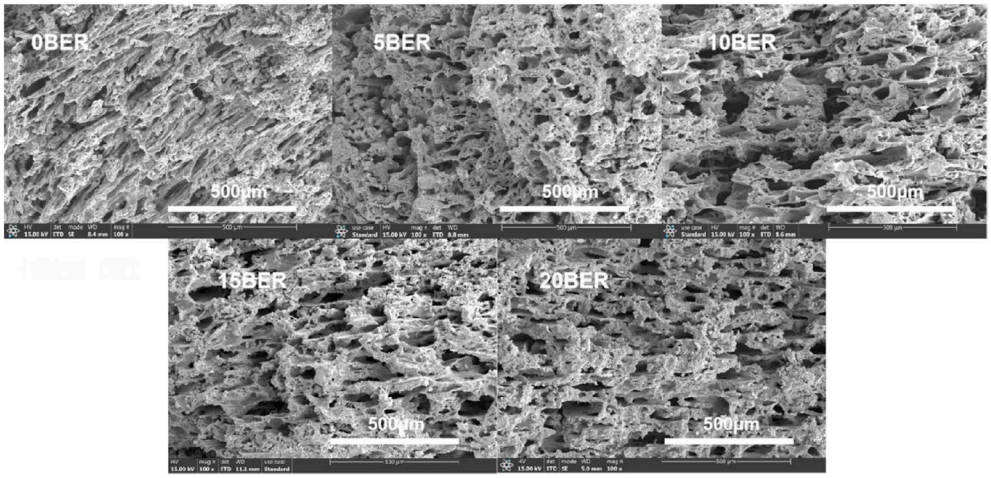

Fig. 9. Sectional morphologies of ceramic layers after ablation.

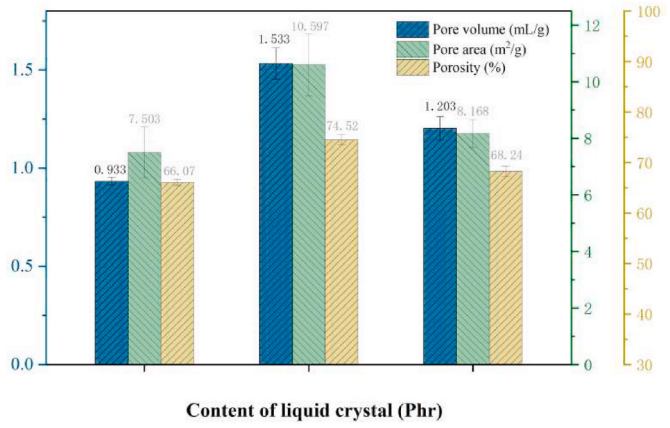

Fig. 10. Pore volumes, porosities and total pore areas of the BER0, BER10 and BER20 samples.

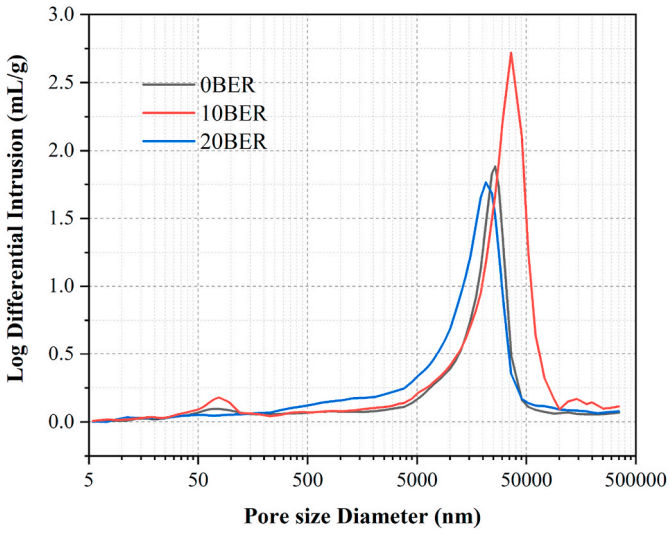

Fig. 11. Pore size distribution of the ceramic layers of the BER0, BER10 and BER20 samples.

orderly structures during pyrolysis. In summary, more ordered structures effectively increased the strength of the ceramic layers, thereby improving the ablation performance of the composites.

3.4. Microscopic morphologies of the silicone rubber composites before and after ablation

The sectional morphologies of the 0BER, 10BER and 20BER composites before ablation is shown in Fig. 8. The broken carbon fibers can be seen in the image. The round protrusions with a diameter of about 3 μm are the SiO_2 nanoparticles. The fibers and their circular cross-section with a diameter of 10 μm are carbon fibers. No obvious BER phase was observed in the composites with the BER component added. This is because epoxy groups existed in both the BER molecules and the epoxy modified silicone rubber matrix. The two components had good compatibility and no phase separation occurred after uniform mixing.

In order to further explore the ablation mechanism of the silicone rubber composites, the sections of the ceramic layers of the sample after ablation were characterized by the microscopic morphology and are shown in Fig. 9. The composites were oxidized from the central area by a large amount of heat energy transferred by the flame, and then the

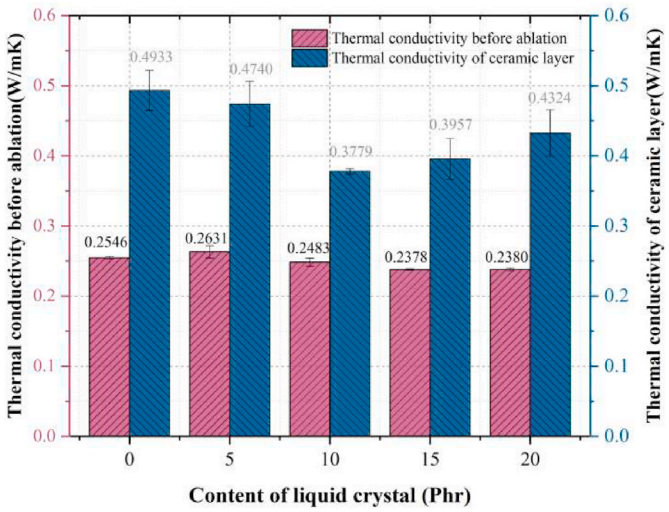

Fig. 12. Thermal conductivities of the silicone rubber composites before and after ablation.

remaining part was carbonized to form dense pores. These holes show a certain degree of order, which is the result of the air flow caused by the high temperature flame. The holes could prevent the flame from spreading to deeper layers of the sample due to their better heat insulation properties.

Due to the number and size of holes could not be visually identified from the SEM images , the mercury intrusion test was used to accurately characterize the pore size and quantities inside the ceramic layers. Fig. 10 shows the pore volumes, porosities and total pore areas of the 0BER, 10BER and 20BER samples. It can be seen that the values of the pore volumes, porosities and total pore areas of three ceramic layers all show a trend of increasing first and then decreasing as the BER composition increases. The 10BER sample had the biggest size and the maximum number of pores. Besides, those of the 20BER are higher than the BER0. Fig. 11 shows the pore size distribution of the ceramic layers of the 0BER, 10BER and 20BER samples. The more log differential intrusion, the bigger pore size. It shows that the 10BER sample has a relatively large pore size, which is consistent with the results in Fig. 10. In addition, the 20BER sample has the widest pore size distribution. The abundant holes effectively reduced the heat transfer of the ceramic layer and prevented the flame from spreading to deeper samples.

The thermal conductivity test was used to characterize the thermal conductivity of the ceramic layers after ablation. Fig. 12 shows the thermal conductivities of the silicone rubber composites before and after ablation. The thermal conductivities of the composites before ablation show no obvious change with the increase of the BER content and are all around 0.25 W/mK. The thermal conductivities of the carbon layers after ablation are increased compared with those before ablation, because the ceramic layers after ablation were composed of carbon residue and ceramic substances with higher thermal conductivity. The thermal conductivities of the ceramic layers added with the BER component are lower than those of the material without BER. With the increase of the BER content, the thermal conductivities of the ceramic layers after ablation show a trend of first decreasing and then increasing. The ceramic layer of the 10BER sample has the lowest thermal conductivity of 0.3779 W/mK. With reference to the results of the mercury intrusion experiment, it can be inferred that the thermal conductivity of the ceramic layers are closely related to the size and number of pores inside. However, according to the decreasing ablation rates of the five samples, although the size, number and distribution of pores have a certain impact on the ablation rate, they are not critical factors.

3.5. Mechanical properties of the silicone rubber composites

The tensile test was used to characterize the mechanical properties of silicone rubber composites before ablation. One of the stress-strain curves of each sample is displayed in Fig. 13, and the average tensile strengths, elastic modulus and stored energy up to breaking of all ceramic layers are listed in Table 3. It can be seen that the tensile strengths of the silicone rubber composites increased significantly with the increase of the BER content. Compared with the 0BER sample, the tensile strength was increased from 1.509 MPa to 1.534 MPa, 1.673 MPa, 1.912 MPa and 3.372 MPa, respectively. The elastic modulus of samples also showed a general upward trend as the content increased. Besides, the 20BER sample exhibits the highest stored energy up to breaking. The addition of BER components significantly improved the tensile properties of silicone rubber composites. The improved mechanical properties can broaden the wide application prospects of silicone rubber composites.

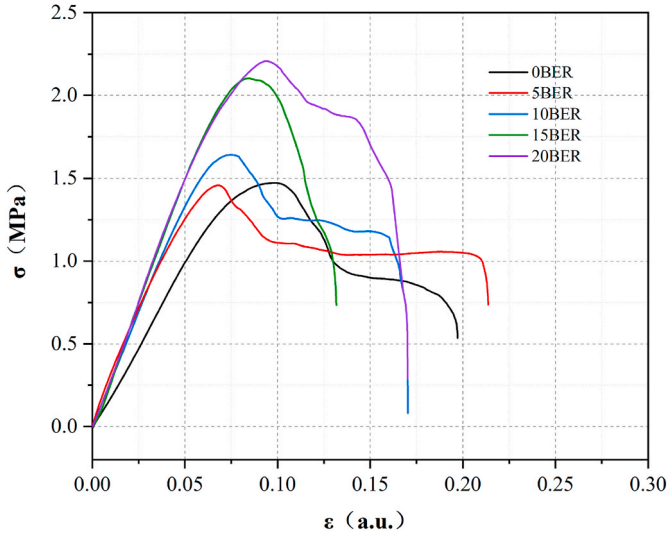

Fig. 13. Stress-strain curves obtained from tensile experiments.

Table 3
Tensile strength and modulus of composites before ablation.

Sample	0BER	5BER	10BER	15BER	20BER
Tensile strength(MPa)	3.768	4.991	7.726	10.339	13.150
Elastic modulus(MPa)	14.959	21.419	21.909	24.813	23.665
Stored energy up to breaking (MPa)	0.1865	0.2196	0.1923	0.1802	0.2597

4. Conclusion

In this study, a series of BER modified silicone rubber ablation composites were prepared by melting, mixing and cold pressing. The ablation resistance of composites was investigated by ablation tests and characterization for the ablated samples. The average linear ablation rate of BER20 was reduced by 54.7% and the average mass ablation rate was reduced by 30.0% compared to the 0BER. The ceramic layers and the material matrix were firmly bonded and the ceramic layers were completely peeled off from the substrate. XRD measurement proved that the ceramization reaction occurred during the ablation process and the ceramic substance SiC was produced. SEM, mercury intrusion and thermal conductivity measurement indicated that the ceramic layers with the BER component had bigger pore volume, porosity and total pore area than the 0BER. The holes made the ceramic layers had better heat insulation properties and could prevent the flame from spreading to deeper parts of the sample. Compression and raman measurement indicated that the addition of BER led to more orderly graphitic carbon structures during pyrolysis and increased the strength of the ceramic layers, which was the key reason for the improvement of the ablation performance of the composites system. In addition, the addition of BER components significantly improved the tensile properties of silicone rubber composites. The improvement of the above properties gives the silicone rubber composites a wide range of application prospects and have the potential to be applied to the surface coating of aircraft.

Notes

The authors declare no competing financial interest.

Data availability

The raw/processed data required to reproduce these findings cannot be shared at this time as the data also forms part of an ongoing study.

CRediT authorship contribution statement

Zhuodong Liu: Investigation, Resources, Writing – original draft, Preparation. **Ziyang Chen:** Data curation, Writing – original draft. **Liwei Yan:** Visualization, Investigation. **Yang Chen:** Conceptualization, Writing – review & editing. **Mei Liang:** Software, Validation. **Huawei Zou:** Project administration.

Declaration of competing interest

The authors of "Ordered graphitized ceramic layer induced by liquid crystal epoxy resin in silicone rubber composites with enhanced ablation resistance performance" declare no competing financial interest.

Acknowledgements

The authors thank the National Natural Science Foundation of China (51703137), Fund project of equipment pre-research field (61409220207) and Key Laboratory of advanced functional composite technology (6142906200111).

References

[1] J. Xiao, J.-M. Chen, H.-D. Zhou, Q. Zhang, Study of several organic resin coatings as anti-ablation coatings for supersonic craft control actuator, Mater. Sci. Eng. 452–453 (2007) 23–30, https://doi.org/10.1016/j.msea.2006.10.020.
[2] M. Natali, J.M. Kenny, L. Torre, Science and technology of polymeric ablative materials for thermal protection systems and propulsion devices: a review, Prog. Mater. Sci. 84 (2016) 192–275, https://doi.org/10.1016/j.pmatsci.2016.08.003.
[3] Y. Zhang, B. Yang, P. Zhang, J. Zhang, J. Ren, Z. Hu, SiC nanowire toughened ZrB2–SiC ablative coating for SiC coated C/C composites, Ceram. Int. 41 (10, Part B) (2015) 14579–14584, https://doi.org/10.1016/j.ceramint.2015.07.175.
[4] J. Mansouri, R.P. Burford, Y.B. Cheng, Pyrolysis behaviour of silicone-based ceramifying composites, Mater. Sci. Eng. 425 (1) (2006) 7–14, https://doi.org/10.1016/j.msea.2006.03.047.
[5] D.W. McKee, C.L. Spiro, E.J. Lamby, The inhibition of graphite oxidation by phosphorus additives, Carbon 22 (3) (1984) 285–290, https://doi.org/10.1016/0008-6223(84)90172-6.
[6] K. Hayashida, S. Tsuge, H. Ohtani, Flame retardant mechanism of polydimethylsiloxane material containing platinum compound studied by analytical pyrolysis techniques and alkaline hydrolysis gas chromatography, Polymer 44 (19) (2003) 5611–5616, https://doi.org/10.1016/S0032-3861(03)00622-0.
[7] J. Gao, Z. Li, J. Li, Y. Liu, Ablation behavior of silicone rubber-benzoxazine-based composites for ultra-high temperature applications, Polymers 11 (11) (2019), https://doi.org/10.3390/polym11111844.
[8] M. Imiela, R. Anyszka, D.M. Bieliński, Z. Pędzich, M. Zarzecka-Napierała, M. Szumera, Effect of carbon fibers on thermal properties and mechanical strength of ceramizable composites based on silicone rubber, J. Therm. Anal. Calorim. 124 (1) (2015) 197–203, https://doi.org/10.1007/s10973-015-5115-x.
[9] Y. Liu, C. Ma, Y. Li, Z. Yin, Y. Zhi, J. Gao, Ablative properties and mechanisms of hot vulcanised silicone rubber (HVSR) composites containing different fillers,

Plastics, Rubber and Composites 45 (10) (2016) 430–435, https://doi.org/10.1080/14658011.2016.1243507.
[10] D. Yang, W. Zhang, B. Jiang, Y. Guo, Silicone rubber ablative composites improved with zirconium carbide or zirconia, Compos. Appl. Sci. Manuf. 44 (2013) 70–77, https://doi.org/10.1016/j.compositesa.2012.09.002.
[11] Q. Pang, F. Kang, J. Deng, L. Lei, J. Lu, S. Shao, Flame retardancy effects between expandable graphite and halloysite nanotubes in silicone rubber foam, RSC Adv. 11 (23) (2021) 13821–13831, https://doi.org/10.1039/d1ra01409a.
[12] L. Lisuzzo, M.R. Caruso, G. Cavallaro, S. Milioto, G. Lazzara, Hydroxypropyl cellulose films filled with halloysite nanotubes/wax hybrid microspheres, Ind. Eng. Chem. Res. 60 (4) (2021) 1656–1665, https://doi.org/10.1021/acs.iecr.0c05148.
[13] G. Cavallaro, G. Lazzara, S. Milioto, F. Parisi, F. Ruisi, Nanocomposites based on esterified colophony and halloysite clay nanotubes as consolidants for waterlogged archaeological woods, Cellulose 24 (8) (2017) 3367–3376, https://doi.org/10.1007/s10570-017-1369-8.
[14] D. Yang, W. Zhang, B. Jiang, Ceramization and oxidation behaviors of silicone rubber ablative composite under oxyacetylene flame, Ceram. Int. 39 (2) (2013) 1575–1581, https://doi.org/10.1016/j.ceramint.2012.07.109.
[15] B. Li, P. Kang, H. Gou, G. Wu, Microstructure and ablation mechanism of graphite/SiC composites under oxy-acetylene flame, Ceram. Int. 40 (4) (2014) 5497–5505, https://doi.org/10.1016/j.ceramint.2013.10.138.
[16] M. Natali, M. Monti, D. Puglia, J.M. Kenny, L. Torre, Ablative properties of carbon black and MWNT/phenolic composites: a comparative study, Compos. Appl. Sci. Manuf. 43 (1) (2012) 174–182, https://doi.org/10.1016/j.compositesa.2011.10.006.
[17] S.J. Ko, G.H. Lee, Y.C. Shin, W.I. Lee, S.H. Yum, H. Kim, Improvement of ablation resistance of epoxy composites reinforced with low concentrations of multi walled carbon nanotubes, Compos. Appl. Sci. Manuf. 124 (2019), https://doi.org/10.1016/j.compositesa.2019.105471.
[18] S.J. Ko, G.H. Lee, Y.C. Shin, W.I. Lee, S.H. Yum, H. Kim, Improvement of ablation resistance of epoxy composites reinforced with low concentrations of multi walled carbon nanotubes, Compos. Appl. Sci. Manuf. 124 (2019) 105471, https://doi.org/10.1016/j.compositesa.2019.105471.
[19] B.-G. Choi, H.-K. Choi, J.-H. Choi, J.-S. Choi, Synthesis and curing behavior of crystalline biphenyl epoxy resin, Korean Chemical Engineering Research 58 (1) (2020) 44–51, https://doi.org/10.9713/kcer.2020.58.1.44.
[20] V. Bermudez, A.A. Ogale, Adverse effect of mesophase pitch draw-down ratio on carbon fiber strength, Carbon 168 (2020) 328–336, https://doi.org/10.1016/j.carbon.2020.06.062.
[21] H. Niu, P. Zuo, W. Shen, S. Qu, Evaluating multi-step oxidative stabilization behavior of coal tar pitch-based fiber, J. Appl. Polym. Sci. (2020), https://doi.org/10.1002/app.50002.
[22] G. Yuan, Z. Xue, Z. Cui, A. Westwood, Z. Dong, Y. Cong, J. Zhang, H. Zhu, X. Li, Constructing the bridge from isotropic to anisotropic pitches for preparing pitch-based carbon fibers with tunable structures and properties, ACS Omega 5 (34) (2020) 21948–21960, https://doi.org/10.1021/acsomega.0c03226.
[23] S.S. Tzeng, Y.G. Chr, Evolution of microstructure and properties of phenolic resin-based carbon/carbon composites during pyrolysis, Mater. Chem. Phys. 73 (2–3) (2002) 162–169, https://doi.org/10.1016/s0254-0584(01)00358-3.
[24] Z.J. Wang, D.J. Kwon, G.Y. Gu, W.I. Lee, J.K. Park, K.L. DeVries, J.M. Park, Ablative and mechanical evaluation of CNT/phenolic composites by thermal and microstructural analyses, Compos. B Eng. 60 (2014) 597–602, https://doi.org/10.1016/j.compositesb.2013.12.042.